Thermochimica Acta, 73 (1984) 89–100
Elsevier Science Publishers B.V., Amsterdam – Printed in The Netherlands

THERMOELECTROMETRY. A REVIEW OF RECENT THERMAL ANALYSIS APPLICATIONS *

W.W. WENDLANDT

Department of Chemistry, University of Houston, Houston, Texas 77004 (U.S.A.)

(Received 3 August 1983)

ABSTRACT

A review of the thermoelectrometry techniques of electrical conductivity, dielectric constant and others. These techniques are not widely employed in thermal analysis but they are useful for certain specific applications. In many cases, the thermoelectrometry measurements are several orders of magnitude more sensitive than DSC or TG. Frequently, these techniques yield data that are of a more fundamental nature than other thermal analysis methods.

INTRODUCTION

According to the International Confederation for Thermal Analysis (ICTA), the thermal analysis technique of thermoelectrometry is defined as "a technique in which the electrical characteristics of a substance is measured as a function of temperature whilst the substance is subjected to a controlled temperature programme" [1]. The most common measurements are of resistance, conductance and capacitance. Thus, thermoelectrometry is not one technique but a series of techniques each of which involves a specific electrical parameter measurement.

Thermoelectrometry techniques are not widely employed in thermal analysis, in fact, they may be described as "neglected" techniques in comparison with the widely used thermogravimetry (TG), differential thermal analysis (DTA) and differential scanning calorimetry (DSC) techniques. Nevertheless, they are important for certain specific applications, many of which will be discussed in this short review.

In a recent thermal analysis technique survey of *Thermochimica Acta* (TCA) and *Journal of Thermal Analysis* (JTA), Wendlandt [2,3] found that thermoelectrometry (electrical properties) accounted for 2.2% of all the

* Presented in part at the Joint Nordic–German Symposium on Thermal Analysis and Calorimetry, Copenhagen, Denmark, August 24–26, 1983.

0040-6031/84/$03.00 © 1984 Elsevier Science Publishers B.V.

techniques used in TCA and 1.4% of the techniques used in JTA. The time period covered by this survey included Volumes 24–29 of TCA and Volumes 8–13 of JTA. This is quite small when compared to 22.0–29.1% for TG and 16.7–26.2% for DTA during the same time frame.

Thermoelectrometry has been briefly reviewed in recent book chapters and articles. Book chapters include those by Wendlandt [4,5] and Warfield [6], and articles by Chiu [30], Paulik and Paulik [7] and Wendlandt [8]. Since most of the thermoelectrometry studies involve simultaneous methods with other thermal analysis techniques, ref. 7 is especially useful.

The purpose of this review is to summarize briefly recent applications (past 10–15 years) of thermoelectrometry and perhaps to stimulate application of these techniques to other thermal analysis problems. Wendlandt [8] has recently summarized the contributions of his laboratory to this area; these applications will not be repeated here. The subject matter of this review will be divided according to the principal electrical parameter measured, namely (a) conductance and resistance; (b) dielectric constant and capacitance; and (c) miscellaneous.

ELECTRICAL CONDUCTANCE AND RESISTANCE

Adeosun and co-workers studied the electrical conductance and other properties of molten lead dodecanoate and mixtures with lead acetate [9], dodecanoic acid [10], metal dodecanoates [11], and lead(II) oxide [12]. Using the specific conductance of lead dodecanoate mixtures, the curvature of these curves were interpreted in terms of a simple dissociation theory involving lead dodecanoate (PbA_2)

$$PbA_2 \rightleftarrows Pb^{2+} + 2\ A^-$$

Assuming that the major charge carrier is Pb^{2+} and that it moves by a simple activated process, the following expressions were obtained

$$\log \kappa = \log Q - \frac{\Delta H_\kappa + \Delta H/3}{2.303RT}$$

and

$$\log Q = \log(NeA/2\ V_m) + \frac{1}{2.303R}\left(\Delta S_\kappa^{\pm} + \frac{\Delta S}{3}\right)$$

where $\Delta H_\kappa^{\pm}$, $\Delta S_\kappa^{\pm}$, ΔH and ΔS are the enthalpies and entropies of activation for movement of the Pb^{2+} ion and the dissociation reaction, respectively. Thus, plots of log κ vs. $1/T$ should be linear with slopes of $(\Delta H_\kappa^{\pm} + \Delta H/3)/2.303R$. For the mixtures of PbA_2 with $Pb(C_2H_3O_2)_2$, the values of $(\Delta H_\kappa^{\pm} + \Delta H/3)$ ranged between 47–50 kJ mol^{-1}.

The dc electrical conductivity of a number of *N*(2-pyridyl)benzamide and

N,*N*′-dibenzoyl-2,6-diaminopyridine metal complexes, as a function of temperature (to 388 K) and γ-radiation, was studied by Abou Sekkina et al. [13]. Linear log σ vs. $1/T$ plots were obtained for all of the Cu(II) and Ni(II) complexes, from which the activation energy, E_a, and other parameters could be calculated, using the expression

$$\sigma = \sigma_0(e^{-E_a/2kT})$$

where σ is the specific conductivity, σ_0 is a constant independent of temperature, k is the Boltzmann constant, and E_a the activation energy (eV). The behavior of a positive temperature coefficient of σ indicates that semiconducting behavior or promotion of electrons from the ground state to excited states may occur. Carrier mobilities, μ, of the different complexes were found to be in the range 10^{-6}–10^{-10} $cm^2\ V^{-1}\ s^{-1}$ and found to increase with an increase in temperature.

Simultaneous thermodilatometry–electrical conductivity measurements have been employed to determine the sintering or coalescence of powdered materials. An equation has been developed by Ramanan and Chaklader [14] which relates electrical conductance to density changes of powder compacts on sintering

$$\Lambda = C\Lambda_0\left[(D/D_0)^{2/3} - 1\right]e^{-E_a/RT}$$

where Λ is the conductance at sample density D, D_0 is the initial density, C is a constant, Λ_0 is the pre-exponential factor, E_a is the activation energy, R is the gas constant and T the temperature. The equation predicts that on heating the powder compact, the conductance should increase rapidly after initial contact between the particles has occurred. To follow both the change in Λ and the shrinkage of the powder compact, simultaneous thermodilatometry–electrical conductance measurements were employed [15–17]. This simultaneous technique has been applied to vitreous materials such as glass, an epoxy resin, iron, $CuSO_4 \cdot 5\ H_2O$, coal ash, and others. The T_g of a vitreous material can be easily obtained using electrical resistance (R) data plotted as a function of $1/T$. The simultaneous dilatometric and electrical resistance curves of $CuSO_4 \cdot 5\ H_2O$ are given in Fig. 1 [17]. Using a compacted sample (to 1500 bars) of the compound, it can be seen that the first four water molecules are evolved in two distinct steps. In addition, the removal of the fifth "water" of hydration appears clearly on the thermodilatometric curve (as it does on the TG and DTG curves) as well as the electrical resistance curve. The fifth molecule is not present as water of hydration but is thought to originate from OH groups in the crystal.

Perhaps the most commonly used simultaneous technique involving electric conductivity is that with DTA. Burmistrova and Fitzeva [18] used this technique to study the reactions between alkaline earth metal oxides (CaO, SrO, BaO) and selected Pb, Cu and Ni halides. Electrical conductivity is useful in determining the appearance of a liquid phase at the moment of

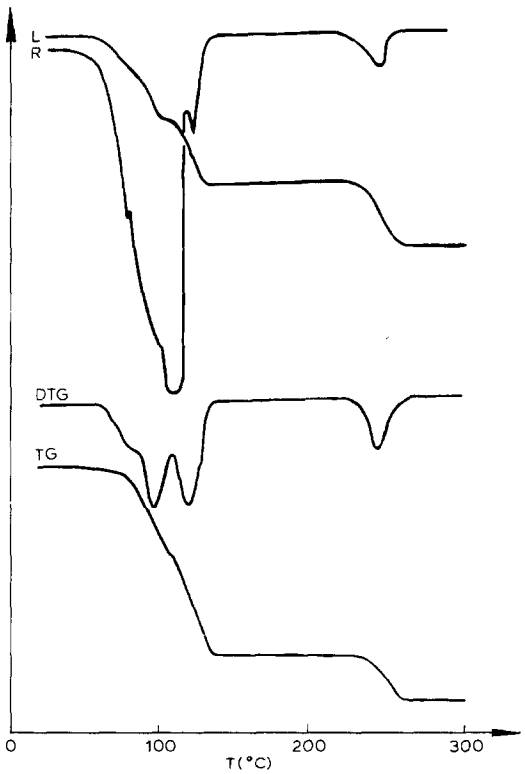

Fig. 1. Simultaneous thermodilatometric (L) and electrical resistance (R) curves of $CuSO_4 \cdot 5 H_2O$. DTG and TG curves are also shown [17].

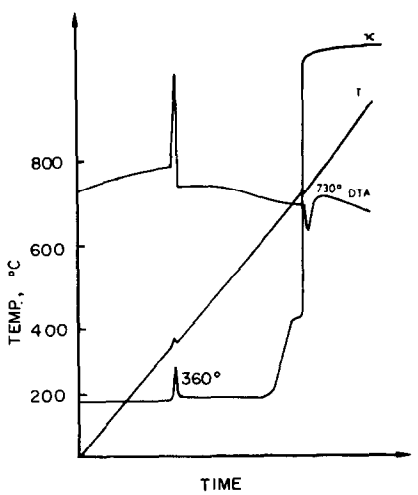

Fig. 2. DTA and electrical conductivity (K) curves for a mixture of BaO and CuBr [18].

interaction between the solids. The interaction between BaO and CuBr, as shown in Fig. 2, is exothermic, as revealed by the DTA curve peak at 360°C. This is also accompanied by an increase in electrical conductivity, forming a small peak in the curve. On further heating, the curve returns to its base line until the reaction product, $BaBr_2$, begins to melt at 730°C, where it again increases rapidly. The 360°C peak, which is due to the melting of the $Ba(OH)_2$–BaO eutectic, also appeared in a reaction mixture of BaO and $PbBr_2$.

Simultaneous electrical conductivity–DTA was used by Romanov et al. [19] to study the thermal behavior of α-oxyalkylphosphanates. It was found that the thermal transformations of these compounds and their analogs are preceded by the ionization of the hydroxy group near the α-carbon atom. On the phosphonate–phosphate rearrangement of α-oxyalkylphosphonates containing electrondonor substituents near the α-carbon atom, no prior decomposition to the initial components takes place, and rearrangement proceeds by an intramolecular tricenter mechanism.

Electrical conductivity was used in conjunction with other thermal analysis techniques by Golunski et al. [20] to study the oxides of antimony. For orthorhombic Sb_2O_3 (valentinite), in N_2, the first thermal effect to be observed by electrical conductivity was a change in slope at about 225°C, which was not observed by any other technique used. This decrease was observed to be the loss of chemisorbed OH groups; the mass-loss being too small to be observed by TG. For cubic Sb_2O_3 (senarmontite), in N_2, changes occurred in the electrical conductivity curve at a temperature well below those observed by DTA or TG. The slope of the electrical conductivity curve increased above 230°C and further changes were observed at 350°C and 530°C, respectively.

Due to the inherent problems of studying the thermal decomposition of NH_4VO_3 by TG and DTA, Trau [21] found that electrical conductivity could be used to provide information relating to the changing concentration of crystal lattice defects. The formation of these lattice defects is connected with any formation process of a new solid phase. A decrease in the electrical conductivity curve in the temperature range 20–50°C was ascribed to the probable desorption of water vapor from the sample surface. Three maxima were observed at 150, 190 and 230°C, respectively, which corresponded well with the three stages of the thermal decomposition process of NH_4VO_3, as determined by other thermal analysis techniques. These maxima can be explained as a result of the decreasing number of lattice defects due to diffusion and combination reactions. A curve peak at 290–370°C was related to the recrystallization of V_2O_5 as well as to the possible oxidation of V_6O_{13} to V_2O_5. The above results show that this technique can be useful for detecting and/or confirming the existence of intermediate products of the thermal decomposition reaction.

This was also the case when Nandi et al. [22] used electrical conductivity

and dielectric constant to study the deaquation reactions of single crystals of $NiSO_4 \cdot 6\ H_2O$ and $NiSO_4 \cdot 7\ H_2O$, as well as $FeSO_4 \cdot 7\ H_2O$ [23] and $CuSO_4 \cdot 5\ H_2O$ [24]. The electrical conductivity curve of a $NiSO_4 \cdot 6\ H_2O$ crystal grown at 40°C contained four distinct peaks at temperature maxima of 100, 142, 186 and 360°C. For $NiSO_4 \cdot 7\ H_2O$ crystals, melting and boiling of the evolved water were also observed in the electrical conductivity curve. One mole of water per mole of salt was evolved from the crystal and dissolved part of the $NiSO_4$, creating Ni^{2+} and SO_4^{2-} ions in solution. These ions caused an increase in conductivity which decreased as boiling began. The number of charged particles, n, in the electrical conductivity curves of these compounds could be determined experimentally by calculating the area under the current vs. time curves and dividing by e, the charge on the electron.

Sircar et al. [25] used electrical conductivity to study carbon filled polymer compounds. Thermal transitions were observed by this technique that could not be detected by any other thermal analysis technique and it could also be used to predict the thermal stability of amorphous polymers. A modified DuPont DSC cell was used for the electrical conductivity measurements. Employing electrical conductivity techniques, Rajeshwar et al. [26] showed that the Green River oil shales decompose by a two-step process in which the rate determining step is (1) breakdown of an outershell polar bridge structure (180–350°C) and (2) cleavage of an inner naphthenic structure also involving polar groups (350–500°C). The observed trend in charge transfer mechanisms in the decomposition behavior of thermally unstable materials may be indicative of how thermal and electrical properties of all solid materials in general are closely coupled.

The ac electrical conductivity of ammonium and alkali metal perchlorates was studied by Rajeshwar et al. [27–29]. Plots of $\ln(\sigma T)$ vs. $1/T$ were made for both heating and cooling cycles with results usually superimposable once the samples were subjected to an annealing treatment. Activation energies were obtained in the usual manner for the K, Cs and Rb salts. The electrical conductivity of ammonium perchlorate is the subject of a major controversy concerning the mechanism controlling charge transfer. One model is that of proton transfer, the other is a defect model in which interstitial NH_4^+ ions are believed to be the dominant charge carrying species. The results of the above investigations are consistent with an extrinsic defect-controlled behavior in the temperature range studied (ambient to 350°C). Identical charge conduction mechanisms were present in all of the perchlorate salts studied. Electrical conduction in the low temperature region is postulated to take place via temperature activated jumps of interstitial cations ($E_a = 0.55$–0.78 eV). Anion vacancies, either free or bound to an impurity ion, contribute appreciably to the conductivity at higher temperatures ($E_a = 0.87$–1.11 eV).

Khilla and Hanna [40] measured the electrical conductivity of CrO_3 from 20 to 182°C. The conductivity decreased with temperature, which may have

been due to the presence of OH^- groups adsorbed on the compound. The activation energy was calculated to be 4.32 eV, which may represent the value for the gap width of CrO_3.

DIELECTRIC CONSTANT

Chiu [30] has described a dielectric apparatus which was used in conjunction with the DuPont 900 thermal analyzer console. This apparatus was used to study the thermal decomposition of selected polymers such as poly(ethyleneterephthalate), poly(vinyl fluoride), poly(vinylidene fluoride), and others. The dielectric constant curves of a group of fluorocarbon polymers are shown in Fig. 3. As given in the figure, the more polar polymers such as poly(vinylidine fluoride) (PVDF) and poly(vinyl fluoride) (PVF) show characteristic dielectric loss peaks which are distinguishable from the relatively featureless and low-loss curves of the other polymers. For PVF, the low temperature process is due to a glass transition while the higher temperature peak is due to a dc conduction mechanism.

Bristoti et al. [31,32] used dielectric constant measurements, as well as other thermal analysis techniques, to study the thermal decomposition of various inorganic compounds. The DTA and dielectric constant curves for $NaNO_3$ both consist of a single peak. In the DTA curve, a narrow endothermic peak centered at 165°C was observed, due to an order–disorder crystalline transition. The dielectric constant curve showed a well defined Debye relaxation behavior for this compound. This relaxation is generally accepted to be due to a diffusion process of the nitrogen ions along the crystal b-axis. It was found that the dielectric constant curve for the dehydration of $CuSO_4 \cdot 5\ H_2O$ was similar to the TG curve rather than the DTA curve of

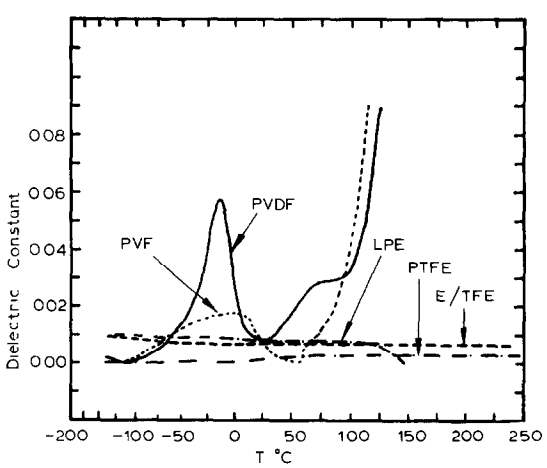

Fig. 3. Dielectric constant curves of various polymers [30].

this compound. The dielectric constant curve for this compound did not show any significant Debye relaxation behavior and changed little during the dehydration reactions.

The dielectric constant curve vs. temperature was also investigated for $K_4[Fe(CN)_6] \cdot 3\ H_2O$ by Bristoti et al. [32] in the temperature range from -80 to 150°C. Four peaks were observed in the curve from -80 to -25°C, due to the presence of the water of hydration. A single peak with a maximum at 105°C was due to a para-electric order–disorder transition. It is in this temperature region that the dehydration reaction

$$K_4[Fe(CN)_6] \cdot 3\ H_2O(s) \rightarrow K_4[Fe(CN)_6]_s + 3\ H_2O(g)$$

takes place.

A novel automated technique for monitoring the frequency and temperature dependence of the ac electrical properties of materials, called Dynamic Dielectric Analysis (DDA), was described by Rajeshwar et al. [33,34]. Extensive use was made of this apparatus to study the thermal properties of $KClO_4$ [33], Green River oil shales [35,36] and oil sands [37]. The weak dependence of ϵ' and ϵ'' on shale organic content at frequencies in the range of 50 Hz to 1 MHz effectively rules out the application of dielectric techniques as an assay tool [35]. The transparent behavior of oil shale minerals to electromagnetic radiation in the microwave frequency could, however, facilitate possible determination of organic content at these frequencies. For oil sands [37], the ϵ' values showed an anomalous increase at temperatures above 200°C and reached a maximum at temperatures in the range 350–450°C. This increase is attributed to polarization effects arising from the thermal decomposition of oil sand bitumen. The dielectric loss tangent ($\tan \delta$) showed a temperature dependence similar in nature to that of ϵ'. This increase in $\tan \delta$ is due to the increased conductivity arising from the creation of mobile charges from thermal fragmentation of the oil sand bitumen. This anomalous increase is superimposed upon the usual exponential temperature dependence of the dc electrical conductivity. Dipolar relaxation effects were observed in $\tan \delta$ (or ϵ'') at temperatures above 150°C. These relaxation effects arise from orientation of dipolar charges created by the thermal decomposition reaction.

The dielectric constant vs. temperature curves of *trans*-stilbene and *N*-benzylideneaniline were determined by Kwatra et al. [38]. As shown by the curve for the latter compound in Fig. 4, the steep curvature of the curve just before melting is indicative of a pre-melting phenomenon involving a solid–solid transition while the behavior in the supercooled region indicates the occurrence of a pre-freezing transition in the liquid state. Such a phenomenon is not uncommon, particularly in molecules with a strong dipolar character, with groups involving torsional oscillations or rotational movements.

The dielectric constant at 1 MHz showed an anomaly near the phase transition point for K_2SO_4 [39]. A gradual increase of the dielectric constant

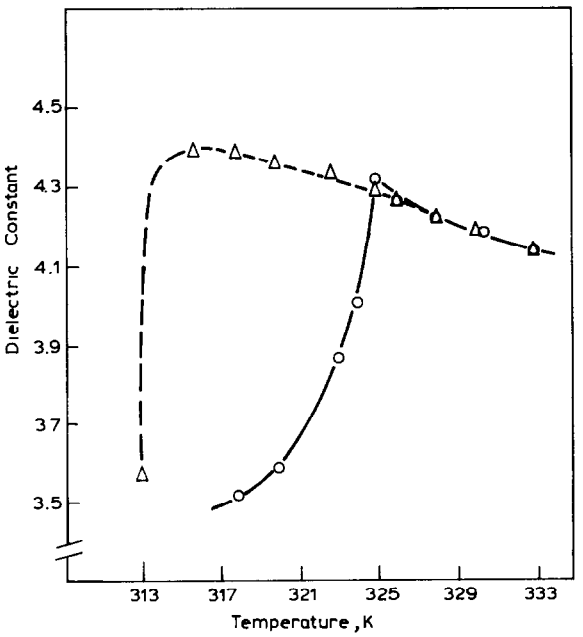

Fig. 4. Dielectric constant of *N*-benzylideneaniline. ○, Heating; △, cooling [38].

at 1 kHz for this compound was observed from 158 to 600°C; at 600°C, the dielectric constant was 469. The temperature dependence of the dielectric constant at 1 MHz above and below 587°C revealed a Curie law behavior.

MISCELLANEOUS ELECTRICAL TECHNIQUES

A current–voltage technique was developed by Rajeshwar [41] to study oil shales. When an electric field is applied to a solid substance, the current flowing through it is time-dependent. Two types of polarization mechanisms have been used to explain this time-dependency, i.e. linear polarization and non-linear polarization. A convenient method of distinguishing between these is to examine the $\ln J_\infty$ vs. $\ln V$ plots (where J_∞ is current density and V is the voltage). Linear polarization will result in curves with a slope of $+1$ whereas non-linear polarization will give linear $\ln J_\infty$ vs. $\ln V$ plots of slope > 1. The oil shales reveal a complex behavior involving both linear and non-linear polarization effects.

A typical current density vs. voltage curve for a Colorado oil shale is given in Fig. 5. An increase in temperature enhanced the non-linearity in the curve while an increase in the shale organic content (or oil yield) tended to enhance the non-linearity of the current–voltage behavior. This was manifested by the shift in the threshold voltage to lower values with increasing oil yield at a given temperature.

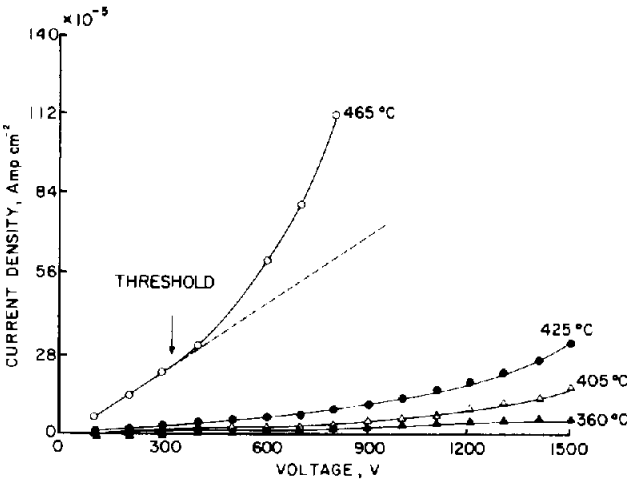

Fig. 5. Variation of current density with voltage for a Colorado oil shale (oil yield = 200 l ton^{-1}) [41].

A new simultaneous thermal analysis technique was reported by Weber and Vogel [42], which consisted of DSC or DTA combined with thermally stimulated discharge (TSD). For copolymers of methyl methacrylate, the molecular origin of the TSD–current at the low temperature side of the T_g was related to the disorientation of small polar segments of the comonomer in the main chain of the polymer. The TSD–current of the α_2-relaxation ($T \sim 80°C$) increased with increasing comonomer content. The TSD_ζ-peak at $T > T_g$ could be attributed to trapped space charges which regain their freedom of motion. This simultaneous technique is recommended for the investigation of the relationship between the dipolarization of dipoles, carrier transport, trapping of real charges and thermal transitions of polymers.

Pillai et al. [43] studied the current vs. temperature curves that were obtained when certain polymers, in contact with two dissimilar metal electrodes, were heated to moderate temperatures. The magnitude of this current was proportional to the metal electrode work function, the liberated ions that reacted with the metal electrodes electrochemically, and the resistance of the cell. A plot of current vs. temperature for cellulose, using Cu–Al electrodes, contained only a single peak in the 50–130°C temperature range. This peak was attributed to the water which was desorbed during the thermal degradation reaction. A second increase in the current above 150°C was attributed to water dehydrated from equatorial hydroxy groups in the cellulosic units. Similar current–temperature curves were obtained on poly(vinyl alcohol) and $NiSO_4 \cdot 6\ H_2O$.

Wendlandt [44] has developed a similar technique but plotted the EMF generated by the reaction with the dissimilar electrodes vs. temperature. Since this was potentially a new general thermal analysis technique, he proposed the name thermovoltaic detection (TVD) for it. The technique was

applied to polymers, organic and inorganic materials, coal, clays and so on [45] and amino acids [46] by Wendlandt and co-workers.

MacKenzie [47,48] has developed a method for the TG study of solids in the presence of applied electrical fields. Electric fields of the order of $\sim 10^5$ V m^{-1} lower the initial decomposition temperature for the dehydroxylation of kaolinite by 60°C in some cases. The activation energy for the process is reduced by 3–12 kcal mol^{-1}. Rate constants for the material are increased by electrolysis but this effect falls off at higher temperature as the normal processes begin to predominate.

ACKNOWLEDGMENT

The financial support of this work by the Robert A. Welch Foundation of Houston, Texas, is gratefully acknowledged.

REFERENCES

1 G. Lombardi, For Better Thermal Analysis, ICTA, Rome, 1977, 19.
2 W.W. Wendlandt, Thermochim. Acta, 36 (1980) 393.
3 W.W. Wendlandt, Natl. Bur. Stand. (U.S.), Spec. Publ. 580, May 1980, 219.
4 W.W. Wendlandt, Thermal Methods of Analysis, Wiley-Interscience, New York, 1964, Chap. XII.
5 W.W. Wendlandt, Thermal Methods of Analysis, 2nd. edn., Wiley-Interscience, New York, 1974, Chap. XII.
6 R.W. Warfield, in I.M. Kolthoff et al. (Eds.), Treatise on Analytical Chemistry, Vol. 4, Part III, Wiley, New York, 1977, p. 608.
7 F. Paulik and J. Paulik, Analyst, 103 (1978) 417.
8 W.W. Wendlandt, Thermochim. Acta, 72 (1984).
9 S.O. Adeosun, Thermochim. Acta, 32 (1979) 119.
10 S.O. Adeosun and M.S. Akanni, Thermochim. Acta, 39 (1980) 35.
11 S.O. Adeosun, M.O. Illori and H.A. Ellis, Thermochim. Acta, 39 (1980) 125.
12 S.O. Adeosun, M.S. Akanni and H.D. Burrows, Thermochim. Acta, 42 (1980) 233.
13 M.M. Abou Sekkina, T.M. Salem, M.F. El-Shazly and A. El-Dissouky, Thermochim. Acta, 48 (1981) 1.
14 T. Ramanan and J. Chaklader, J. Am. Ceram. Soc., 58 (1975) 476.
15 E. Raask, Stanton-Redcroft Application Note 253, Stanton-Redcroft, London.
16 E. Karmazsin, M. Romand and M. Murat, Proc. 2nd European Symp. on Thermal Analysis, D. Dollimore (Ed.), Sept. 1–4, 1981, Heyden, London, 562 pp.
17 E. Karmazsin, M. Romand and M. Murat, Thermochim. Acta, 55 (1982) 293.
18 N.P. Burmistrova and R.G. Fitzeva, J. Thermal Anal., 4 (1972) 161.
19 G.V. Romanov, R.G. Fitzeva, I.V. Konovalova, A.N. Pudovik and N.P. Burmistrova, J. Thermal Anal., 6 (1974) 119.
20 S.E. Golunski, T.G. Nevell and M.I. Pope, Thermochim. Acta, 51 (1981) 153.
21 J. Trau, J. Thermal Anal., 6 (1974) 355.
22 P.N. Nandi, D.A. Deshpande and V.G. Kher, Thermochim. Acta, 34 (1979) 1.
23 P.N. Nandi, D.A. Deshpande and V.G. Kher, Indian J. Pure Appl. Phys., 16 (1978) 742.

24 P.N. Nandi, D.A. Deshpande and V.G. Kher, Proc. Indian Acad. Sci., Sect. A, 88 (1979) 113.
25 A.K. Sircar, T.G. Lamond and J.L. Wells, Thermochim. Acta, 37 (1980) 315.
26 K. Rajeshwar, M. Das and J. DuBow, Nature (London), 287 (1980) 131.
27 K. Rajeshwar, R. Nottenburg, V.R. Pai Verneker and J. DuBow, J. Chem. Phys., 72 (1980) 6678.
28 R. Nottenburg, K. Rajeshwar, V.R. Pai Verneker and J. DuBow, J. Phys. Chem. Solids, 41 (1980) 271.
29 K. Rajeshwar, R. Nottenburg, V.R. Pai Verneker and J. DuBow, Phys. Status Solidi, 58 (1980) 245.
30 J. Chiu, Thermochim. Acta, 8 (1974) 15.
31 I.R. Bonilla, P.R. Andrade and A. Bristoti, J. Thermal Anal., 8 (1975) 387.
32 A. Bristoti, I.R. Bonilla and P.R. Andrade, J. Thermal Anal., 9 (1976) 93.
33 R. Nottenburg, M. Freeman, K. Rajeshwar and J. DuBow, Anal. Chem., 51 (1979) 1149.
34 R. Nottenburg, K. Rajeshwar, M. Freeman and J. DuBow, J. Solid State Chem., 28 (1979) 195.
35 R. Nottenburg, K. Rajeshwar, M. Freeman and J. DuBow, Thermochim Acta, 31 (1979) 39.
36 K. Rajeshwar, J. DuBow and R. Thapar, Can. J. Earth Sci., 17 (1981) 1315.
37 M. Das, R. Thapar, K. Rajeshwar and J. DuBow, Can. J. Earth Sci., 18 (1981) 742.
38 B. Kwatra, V. Ramakrishna and S.K. Suri, Thermochim. Acta, 48 (1981) 231.
39 T. Watanabe, K. Sakai and S. Iwai, Bull. Tokyo Inst. of Technol., 117 (1973) 13.
40 M.A. Khilla and A.A. Hanna, Thermochim. Acta, 51 (1981) 335.
41 K. Rajeshwar, Thermochim. Acta, 54 (1982) 59.
42 G. Weber and B. Vogel, Angew. Makromol. Chem., 86 (1980) 215.
43 P.K.C. Pillai, S.F. Xavier and M. Mollah, Thermochim. Acta, 35 (1980) 385.
44 W.W. Wendlandt, Thermochim. Acta, 37 (1980) 121.
45 W.W. Wendlandt and S. Contarini, Thermochim. Acta, 65 (1983) 321.
46 S. Contarini and W.W. Wendlandt, Thermochim. Acta, 70 (1983) 283.
47 K.J.D. MacKenzie, J. Thermal Anal., 5 (1973) 5.
48 K.J.D. MacKenzie and N. Hadipour, Thermochim. Acta, 35 (1980) 227.